Experimental Observations of Nonlinear Saturation of the Two-Plasmon Decay Instability

H. A. Baldis and C. J. Walsh
Division of Physics, National Research Council, Ottawa, Ontario K1A 0R6, Canada
(Received 31 August 1981)

Direct measurements by time-resolved Thomson scattering of the saturation of the two-plasmon decay instability driven by a CO_2 laser in an underdense plasma are presented. A time-correlated growth in ion fluctuations is also seen, enabling the saturation mechanism to be identified with the ion motions driven by the ponderomotive force associated with the large-amplitude electrostatic waves.

PACS numbers: 52.35.Py, 52.25.Ps

In the coupling of laser energy to a plasma, an understanding of the parametric instabilities which may occur is important, particularly when an electrostatic wave is produced in the decay. Large-amplitude electron waves can accelerate electrons, producing heated electron distributions which may have detrimental effects in laser fusion schemes. Consequently, mechanisms capable of saturating the amplitudes of these driven waves are also of importance.

The decay of the incident electromagnetic wave into two electrostatic waves[1,2] (the two-plasmon decay), which is an absolute instability occurring at quarter-critical density, is of current interest. Its occurrence has been demonstrated experimentally, both by emission[3] at $\frac{3}{2}\omega_0$ and more directly by the observation, with use of Thomson scattering,[4] of large-amplitude electron plasma waves at $n_c/4$. The generation of high-energy electron distributions by this instability has been observed in both simulation[5] and experiment.[6]

Several theoretical predictions have been made for mechanisms by which the instability might saturate. These include nonlinear damping,[7] pump depletion,[2] and mechanisms due to ponderomotive effects, including those of profile steepening,[5] soliton formation,[8] and coupling of the electrostatic waves to shorter-wavelength ion fluctuations.[5] In this paper, we present the results of an experiment carried out with an intense 10.6-μm (CO_2) laser, using the technique of time-resolved Thomson scattering,[9] which has allowed the temporal evolution of both the electrostatic wave amplitude produced by the instability, and ion motions produced by mode coupling,[5] to be observed. In this way the saturation of the instability and the mechanism responsible have been identified.

The experiment was carried out with use of a CO_2 laser, with energies from 0.2 to 30 J in a ~1-ns pulse ($10^{12} \lesssim I \lesssim 1.5\times10^{14}$ W cm^{-2}) incident upon a preformed plasma with $T_e \lesssim 100$ eV and a scale length $L=(d\ln n/dx)^{-1}\sim 30\lambda_0$ in the density range $n/n_c \sim 0.1$–2, where λ_0 is the vacuum wavelength of the CO_2 laser. The arrangement has been discussed in detail elsewhere.[6] The main features are shown in Fig. 1. The scattering diagnostic, which used a 0.53-μm probe synchronized to the CO_2 laser, is also shown in Fig. 1. The geometry of the scattering optics was designed to probe for those plasma waves most strongly excited by the $2\omega_p$ instability. The scattered signal was analyzed with use of a spectrograph in combination with a streak camera and recorded either with a high-gain vidicon system or with 35-mm film.[9] The data thus obtained had a time resolution ~40 ps and a spectral resolution $\lesssim 10$ Å. In order to measure the electron density, interferometry was performed every shot. Only those shots for which $n_e \sim 0.25 n_c$ in the interaction region were analyzed.

For the scattering geometry of this experiment,

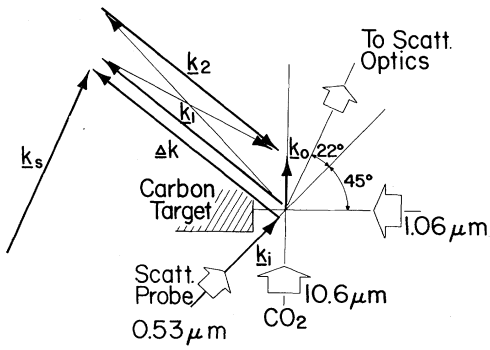

FIG. 1. Geometry of the experiment. The plasma is formed by ablation from the carbon target with use of a Q-switched 1.06-μm laser. The CO_2 laser is incident at 90° to the axis of the plasma plume. $\vec{k}_0$ is the CO_2 wave vector. $\vec{k}_i$ and $\vec{k}_s$ are the wave vectors of the incident (0.53 μm) and scattered light. $\Delta\vec{k}=\vec{k}_s-\vec{k}_i=\vec{k}_1=-\vec{k}_2$ is the plasma wave vector probed. k_1 and k_2 are close to the wave vectors of maximum growth rate for the $2\omega_p$ instability.

the parameter $\alpha=(\Delta k\lambda_D)^{-1}\sim 6-10$. The spectrum will thus consist of a central ion peak and two electron satellites,[10] separated by ~125 Å from the central component when $n_e=n_c/4$. The ratio of the signal in the electron and ion features is given as $S_e/S_i\sim[2(1+\alpha^2)]^{-1}\sim 10^{-2}$ for a thermal plasma. This is essentially a measure of the fluctuation amplitudes of the ion and electron waves in this range of k space. In a plasma where large-amplitude electrostatic waves exist, produced for example by the $2\omega_p$ instability, the electrostatic wave energy may be enhanced by many orders of magnitude above the thermal level. This enhancement will be seen in the scattered spectrum in the electron satellites. In the case of the $2\omega_p$ instability, both satellites will be enhanced, with each generated from separate decay pairs (as indicated by k_1 and k_2 in Fig. 1).

The transition from thermal to nonthermal scattering during the rise time of the CO_2 laser is shown in Fig. 2. Using results like this, obtained at different laser energies, we have been able to make some observations on the behavior of the $2\omega_p$ instability. Strong nonthermal electron fluctuations are seen when $E\gtrsim 0.2$ J. The peak instantaneous amplitude saturates above $E\sim 2$ J (Fig. 3). At low energies, the duration of the observed nonthermal scattering is short ($\lesssim$100 ps). As the energy increases, so does the duration (up to 1 ns for $E\gtrsim 20$ J), but the peak amplitude always occurs towards the beginning of the enhanced signal. These are the points plotted in Fig. 3. The time lag in the observed onset of the nonthermal fluctuations relative to the rise in the CO_2 intensity agrees well with theoretical predictions for the threshold and growth rate of the $2\omega_p$ instability.[2]

At higher incident energies, nonthermal ion fluctuations are also observed (Fig. 4). These always commence after the electron fluctuations. For $E\lesssim 2$ J, the time lag is ~200–400 ps (and sometimes no enhancement of the ion feature occurs). When $E>2$ J, the time lag drops rapidly to ~20–50 ps. Enhanced ion fluctuations are always seen in this energy range. The level of enhancement of the ion feature above thermal fluctuations is $\sim 10^2$ when $E\sim 20$ J.

Figure 5 shows the time evolution of the electron and ion enhanced fluctuations for an incident CO_2 energy ~2 J. The observed maximum in the enhancement takes place during the rise time of the CO_2 laser and not at its peak. There is a clear time correlation between the rise and fall of the electron and ion features.

These results strongly suggest that the saturation behavior observed in Fig. 3 is associated with the coupling of electrostatic wave energy into shorter-wavelength ion fluctuations by ponderomotive effects, as predicted by Langdon,

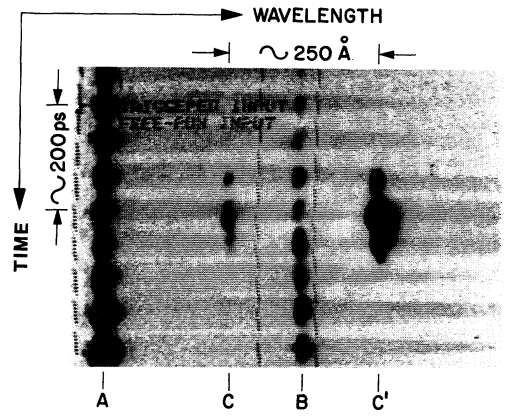

FIG. 2. Thomson scattered light for CO_2 energy = 1 J incident upon the plasma at $0.25n_c$. A is a monitor of the incident probe pulse. B, C, and C' are the ion feature and blue and red electron satellites, respectively. Note that the 80-ps modulation in the scattered-light intensity is due to intensity modulations in the input pulse. The normalized intensity of the scattered light in the ion feature stays constant during the CO_2 laser pulse (which begins shortly after the start of the streak). However, strong nonthermal fluctuations (~ 500 times thermal levels) are seen in the electron satellites for ~ 200 ps around the peak of the laser pulse.

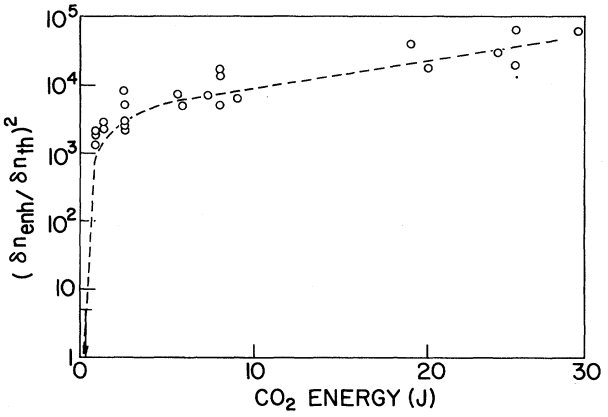

FIG. 3. The peak instantaneous scattered signal of the electron feature (normalized to thermal levels measured in the plasma without the CO_2 laser) as a function of laser energy. Several shots for $\lesssim$ 100 mJ are shown, for which the ratio was $\lesssim 10$. The curve shows strong growth for $E\lesssim 1-2$ J, and saturated growth subsequent to that.

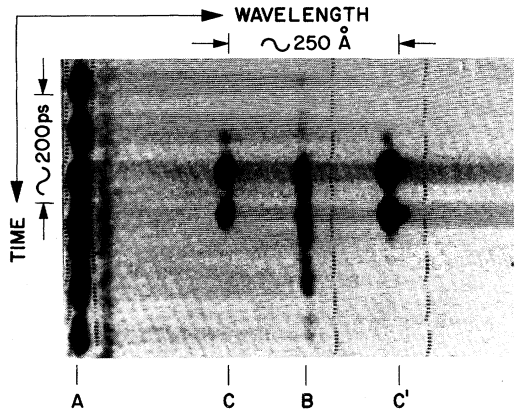

FIG. 4. Thomson scattering for a CO_2 energy of 2 J, higher than that shown in Fig. 2. Both thermal and nonthermal scattering in the ion feature (B) can be seen. Note that the scattered signal has been attenuated with respect to Fig. 2. The onset of nonthermal ion fluctuations lags that in the electron satellites by ~ 50 ps. In this shot, the electron fluctuations were $\sim 2\times 10^3$ times above thermal levels. The ion fluctuations were ~ 5 times above thermal levels.

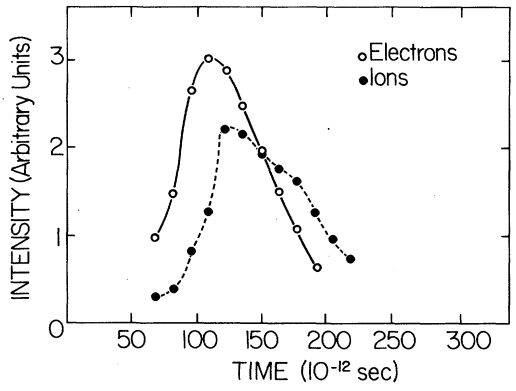

FIG. 5. Normalized microdensitometer data from a streak record showing (1) the abrupt rise and fall of the ion and electron features and (2) their time correlation. The vertical scale indicates the scattered intensity *normalized* to the input probe intensity to remove the effect of probe modulation. The features plotted here occurred before the peak in the CO_2 laser pulse, at the very beginning of a period of nonthermal scattering which lasted for longer than 500 ps. CO_2 energy = 2 J.

Lasinski, and Kruer.[5] Saturation is seen in Fig. 3 when $(\delta n_{enh}/\delta n_{th})^2 \sim 10^3$ ($k\lambda_D \sim 0.2$), and since in our experiment $n\lambda_D{}^3 \sim 10^3$, ponderomotive force effects are indeed expected to be of importance for such electron plasma wave amplitudes.[5] These can be manifested in either shorter-wavelength ion fluctuations (as seen by Thomson scattering in the present experiment) or in profile steeping, as reported previously.[4] However, the time scale required for profile steepening to occur is longer than that necessary to drive up the short-wavelength ion fluctuations by a ratio $\sim 2l/\lambda_{epw}$, where l is the mismatch scale length and λ_{epw} is the wavelength of the electron plasma waves.[5] Since the short-wavelength ion fluctuations occur over a time scale ~20–50 ps (Fig. 5), and $l \gg \lambda_{epw}$, we do not expect profile steepening to play a role in the saturation, at early times, of the electrostatic wave amplitude observed in this experiment. Conversely the strong time correlation between the onset of saturation and the occurrence, within several ion acoustic periods, of the short-wavelength ion fluctuations leads us to an identification of these as the saturation mechanism. The ion and electron plasma waves probed in the experiment are of similar wavelength, whereas the theory of Langdon, Lasinski, and Kruer predicts a coupling of electrostatic waves at wave number k to produce ion waves at $2k$. However, for our experimental conditions the growth spectrum of unstable electron plasma waves is very broad at long wavelengths ($k\lambda_D \ll 1$). Furthermore, on the basis of calculations that use the linear theory,[2] we expect the development of the longer-wavelength electron plasma waves (producing the ion fluctuations) to be the same (within experimental limits) as that of the electron plasma waves observed.

We now discuss briefly the saturation of the electron plasma waves due to electron trapping.[7] The main signature of such a process is the production of a very-high-energy tail in the electron distribution.[5] Such a tail was observed in previous experiments with use of electron spectrometers[6] only for energies in excess of 10 J. This suggests that electron trapping does indeed occur, but at energies for which the growth of the $2\omega_p$ instability is already saturated by the mode-conversion process discussed previously. As for the other mechanisms mentioned previously, pump depletion should not be important because the pump intensity is well above threshold. The possibility of soliton formation[8] would seem to be precluded by the same argument as that against profile steepening: Both processes occur over a time scale much longer than that observed here for saturation to occur.

We acknowledge useful and informative discussions with Dr. A. B. Langdon and Dr. B. F. Lasinski of the Lawrence Livermore National Labora-

tory. The continuing technical assistance of R. Benesch, the assistance of R. W. Sancton with the video recording system, and that of A. Avery with operation of the CO_2 laser are gratefully acknowledged.

[1]M. V. Goldman, Ann. Phys. (N.Y.) 38, 117 (1966); E. A. Jackson, Phys. Rev. 153, 235 (1967).

[2]C. S. Liu and M. N. Rosenbluth, Phys. Fluids 19, 967 (1976); B. F. Lasinski and A. B. Langdon, Laser Program Annual Report— 1977, Lawrence Livermore Laboratory Report No. UCRL-50021-77 (unpublished).

[3]H. C. Pant, K. Eidmann, P. Sachseumaier, and R. Sigel, Opt. Commun. 16, 396 (1976); P. D. Carter, S. M. L. Sim, H. C. Barr, and R. G. Evans, Phys. Rev. Lett. 44, 1407 (1980).

[4]H. A. Baldis, J. C. Samson, and P. B. Corkum, Phys. Rev. Lett. 41, 1719 (1978).

[5]A. B. Langdon and B. F. Lasinski, in *Methods in Computational Physics*, edited by B. Alder, S. Fernbach, and M. Rotenberg (Academic, New York, 1976), Vol. 16; A. B. Langdon, B. F. Lasinski, and W. L. Kruer, Phys. Rev. Lett. 43, 133 (1979).

[6]N. H. Ebrahim, H. A. Baldis, C. Joshi, and R. Benesch, Phys. Rev. Lett. 45, 1179 (1980).

[7]W. L. Kruer and J. M. Dawson, Phys. Fluids 15, 446 (1972).

[8]H. H. Chen and C. S. Liu, Phys. Rev. Lett. 39, 881 (1977).

[9]H. A. Baldis, C. J. Walsh, and R. Benesch, to be published.

[10]J. Sheffield, *Plasma Scattering of Electromagnetic Radiation* (Academic, New York, 1975).

Hard-X-Ray Measurements of 10.6-μm Laser-Irradiated Targets

W. Priedhorsky, D. Lier, R. Day, and D. Gerke

University of California, Los Alamos National Laboratory, Los Alamos, New Mexico 87545

(Received 1 June 1981; revised manuscript received 16 November 1981)

The first measurements of high-energy x-ray emission ($h\nu \sim 30-300$ keV) by high-Z microballoon targets irradiated at $5\times10^{14} < \varphi < 2\times10^{16}$ W/cm^2 by 10.6-μm laser light are reported. An exponential spectrum with a slope $kT_H \sim 250$ keV provides the best fit to spectrometer data at $\varphi_l = 10^{16}$ W/cm^2. The hard-x-ray yield indicates that a substantial fraction, probably between 10% and 100%, of the absorbed laser energy is converted to hot electrons. The slope kT_H is proportional to the fastest ion energy.

PACS numbers: 52.50.Jm, 79.20.Ds

Laser-fusion target performance can be significantly limited by fuel preheat. Energetic electrons created at the laser absorption surface deposit energy in the fuel, preventing efficient compression. The electron distribution may be diagnosed by measurement of high-energy x-ray bremsstrahlung created by electron interaction with the target material. We report the first such measurements of targets irradiated by the 10.6-μm Helios CO_2 laser facility.[1]

The slope of the target hard-x-ray continuum was determined by a least-squares fit to signals from a ten-channel array of broadband filter-scintillator channels spanning the region $h\nu \approx 30$–300 keV. Five of the channel response functions are shown in Fig. 1. Priedhorsky and Lier describe the instrument, and its calibration, analysis, and background tests in detail.[2]

A series of gold- or tungsten-coated solacels (hollow nickel microballoons) were irradiated at a range of focus conditions. The laser energy ranged from 2 to 8 kJ in a 0.75-ns (full width at half maximum) pulse. The targets were 300 and

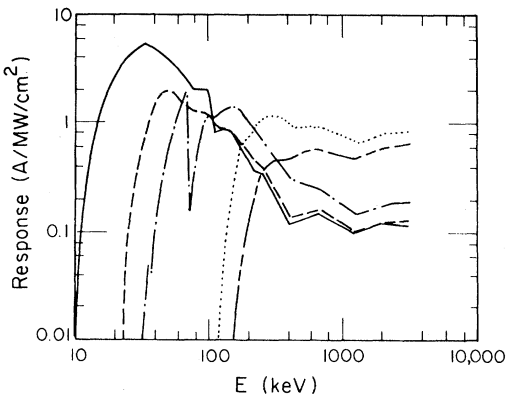

FIG. 1. Five typical spectral response functions from the ten-channel high-energy x-ray spectrometer.

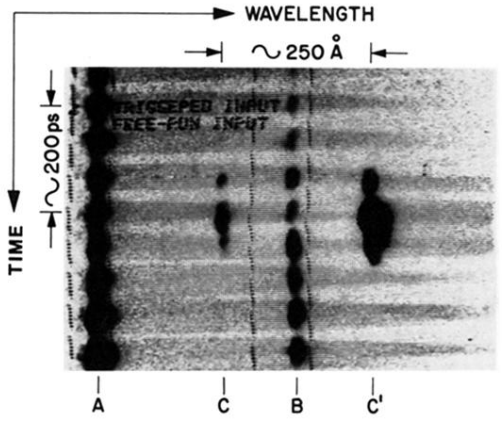

FIG. 2. Thomson scattered light for CO_2 energy = 1 J incident upon the plasma at $0.25n_c$. A is a monitor of the incident probe pulse. B, C, and C' are the ion feature and blue and red electron satellites, respectively. Note that the 80-ps modulation in the scattered-light intensity is due to intensity modulations in the input pulse. The normalized intensity of the scattered light in the ion feature stays constant during the CO_2 laser pulse (which begins shortly after the start of the streak). However, strong nonthermal fluctuations (~ 500 times thermal levels) are seen in the electron satellites for ~ 200 ps around the peak of the laser pulse.

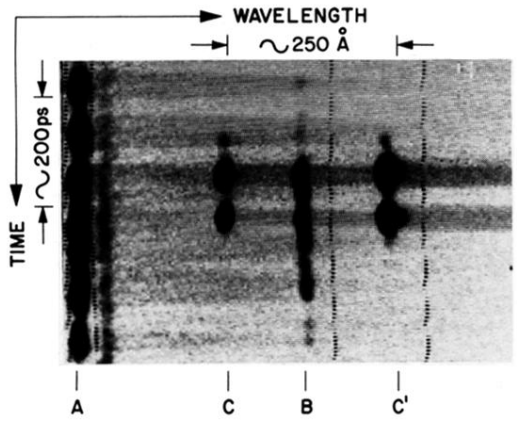

FIG. 4. Thomson scattering for a CO_2 energy of 2 J, higher than that shown in Fig. 2. Both thermal and nonthermal scattering in the ion feature (B) can be seen. Note that the scattered signal has been attenuated with respect to Fig. 2. The onset of nonthermal ion fluctuations lags that in the electron satellites by ~ 50 ps. In this shot, the electron fluctuations were $\sim 2\times 10^3$ times above thermal levels. The ion fluctuations were ~ 5 times above thermal levels.